Received: 10 October 2017 | Revised: 8 December 2017 | Accepted: 10 December 2017

DOI: 10.1002/aoc.4263

FULL PAPER

WILEY Applied Organometallic Chemistry

Preparation of novel palladium nanoparticles supported on magnetic iron oxide and their catalytic application in the synthesis of 2-imino-3-phenyl-2,3-dihydrobenzo[*d*]oxazol-5-ols

Davood Habibi | Somayyeh Heydari | Mina Afsharfarnia | Fatemeh Moghimpour

Department of Organic Chemistry, Faculty of Chemistry, Bu-Ali Sina University, Hamedan 6517838683, Iran

Correspondence
Davood Habibi, Department of Organic Chemistry, Faculty of Chemistry, Bu-Ali Sina University, Hamedan 6517838683, Iran.
Email: davood.habibi@gmail.com

Novel Pd nanoparticles were prepared in five successive stages: 1) preparation of the Fe_3O_4 magnetic nanoparticles (Fe_3O_4 MNPs), 2) coating of Fe_3O_4 MNPs with SiO_2 (Fe_3O_4@SiO_2), 3) functionalization of Fe_3O_4@SiO_2 with 3-chloropropyltrimethoxy- silane (CPTMS) ligand (Fe_3O_4@SiO_2@CPTMS), 4) further functionalization with 3,5-diamino-1,2,4-triazole (DAT) ligand (Fe_3O_4@SiO_2@CPTMS @DAT), and 5) the complexation of Fe_3O_4@SiO_2@CPTMS@DAT with $PdCl_2$ (Fe_3O_4@SiO_2@CPTMS@ DAT@Pd). Then, the obtained Pd nano-catalyst characterized by different methods such as the elemental analysis (CHN), FT-IR, XRD, EDX, SEM, TEM, TG-DTA and VSM. Finally, the Pd catalyst was applied for the synthesis of various 2-imino-3-phenyl-2,3-dihydrobenzo[*d*]oxazol-5-ols.

KEYWORDS
3,5-diamino-1,2,4-triazole, 3-chloropropyltrimethoxysilane, Fe_3O_4 Magnetic nano-particles, Pd complex, SiO_2

1 | INTRODUCTION

Application of Pd catalyst has been extensively studied in organic reactions. For example, F. Liu and coworkers modified the Na^+ montmorillonite with L-cystine, and subsequently Pd was loaded via an ion-exchange reaction under microwave irradiation to obtain the Pd@Mont catalyst. The catalyst was subsequently applied for the Suzuki cross-coupling reaction to obtain the corresponding products in good to excellent yields.[1] N. Telvekar and coworker applied a simple and efficient method for the synthesis 2-phenyl pyridine via cyclization of aryl ketone with 1,3-diaminopropane using $Pd(OAc)_2$ as catalyst.[2] The Pd(II) complexes were obtained by P. Viswanathamurthi and coworker from the reaction of $[PdCl_2(PPh_3)_2]$ with pyridoxal thiosemicarbazone and pyridoxal *N*-methyl thiosemicarbazone, respectively in ethanol. To screen the catalytic properties of the synthesized complexes, Pd(II) complexes catalyzed three-component coupling reaction of aldehydes, amines and phenylacetylenes under solvent free conditions in ionic liquid at 80 °C to give propargylamines in high yields.[3] Trans $[PdCl_2(PPh_3)_2]$ complex was synthesized, characterized and applied by Ali Naghipour and coworker as an efficient catalyst for the amination of aryl halides to afford primary amines and also in the catalytic Stille cross-coupling reaction with satisfactory results.[4] A. M. Trzeciak and coworkers synthesized and characterized two Pd complexes of the type $[PdL_2Cl_2]$ containing chiral imidazole ligands (L = 1-bornyloxymethylene imidazole or 1-fenchyloxymethylyne imidazole) were synthesized. They tested the two obtained catalysts in various C-C bond forming reactions, namely Suzuki–Miyaura, carbonylative Suzuki–Miyaura, asymmetric Heck-type coupling reactions and asymmetric conjugate addition of phenylboronic acid to heterocyclic acceptors.[5] U. Bora and coworker prepared the gallic acid-derived Pd(0) nanoparticles catalyst for the Sonogashira reactions in ethanol

 Copyright © 2018 John Wiley & Sons, Ltd.

under optimum thermal conditions.[6] M. Rocamora and coworker prepared series of cationic allyl Pd complexes $[Pd(\eta^3\text{-}CH_3\text{-}C_3H_5)(P\text{-}P)]X$ (X = PF_6 and X = BPh_4) and $[Pd(\eta^3\text{-}1,3\text{-}Ph_2\text{-}C_3H_3)(P\text{-}P)]X$ (X = PF_6 and X = BPh_4) and applied them in the asymmetric allylic substitution reaction of the benchmark substrate *rac*-3-acetoxy-1,3-diphenyl-1-propene with dimethyl malonate and benzylamine as nucleophiles in order to test their catalytic potential.[7] T. E. Klimova and coworker prepared the Pd catalysts supported on hydrogen titanate nanotubes by adsorption of $Pd(OAc)_2$ from CH_2Cl_2 solutions. Catalytic activity was tested in the Heck reaction between 4-bromobenzaldehyde or 4-bromostyrene and styrene. Only the E-isomers of the corresponding cross-coupled products were obtained.[8] B. J. V. Tongol and coworkers synthesized a catalyst consisting of Pd–Ni supported on graphene oxide composite. The catalytic activity was tested for ethanol oxidation reaction in half-cell using cyclic voltammetry and subsequently it used as an anode material in a direct ethanol fuel cell.[9] Polycarbosilane was synthesized by K. Sreekumar and coworker via the polycondensation of trichloromethylsilane and trimethoxyvinylsilane in the presence of sodium metal. Then, $Pd(OAc)_2$ was attached to the polycarbosilane and its catalytic activity investigated in the C–C coupling Heck reaction between aryl halides or vinyl halides and activated.[10]

Since magnetic nanoparticles have a large surface-to-volume ratio, their catalytic activities can be improved significantly.[11–13] Among magnetic nanoparticles, Fe_3O_4 is the most widely used for catalyst supports as it has less toxicity compared to other metallic counterparts.[14]

Herein, we report preparation of a novel Pd nano-particle catalyst via synthesis of the Fe_3O_4 magnetic nanoparticles, its coating with SiO_2, functionalization with 3-chloropropyltrimethoxysilane and 3,5-diamino-1,2,4-triazole ligands, and complexation with $PdCl_2$ (Scheme 1).

Furthermore, in continuation to our synthesis of the nitrogen-containing compounds, we intend to report a mild, efficient and convenient procedure for the synthesis of a range of 2-imino-3-phenyl-2,3-dihydrobenzo[*d*]oxazol-5-ol by the sue of this Pd nano-catalyst in acetonitrile at room temperature (Scheme 2).

2 | EXPERIMENTAL

2.1 | General

All reagents were purchased from the Merck and Aldrich chemical companies and used without further purification. The NMR spectra were recorded in DMSO or $CDCl_3$. ^{1}HNMR and ^{13}C NMR spectra were recorded on a Bruker Avance DRX 400 and 300 MHz instruments. The chemical shifts are reported in parts per million relative to TMS as an internal standard and *J* values are given in hertz. FT-IR (KBr) spectra were recorded on a Perkine Elmer 781 spectrophotometer. Melting points were taken in open capillary tubes with a BUCHI 510 melting point apparatus and are uncorrected. Elemental analysis was performed using Heraeus CHNeO-Rapid analyzer. The ICP measurements for the metal content evaluation were performed using a Perkin-Elmer ICP/6500. TLC was performed on silica gel polygram SIL G/UV 254 plates. The TEM images were recorded on a Zeiss-EM10C-80 KV transmission electron microscope, and the SEM images were recorded on a Philips XL-30 scanning electron microscope. The XRD measurements were done by a Bruker D8 Advance powder diffractometer, using Cu Kα (λ=1.54 A°) as the incident radiation. Magnetic measurements were carried out at room temperature using an Iranian Meghnatis Daghigh Kavir Co Vibrating Sample Magnetometer (VSM).

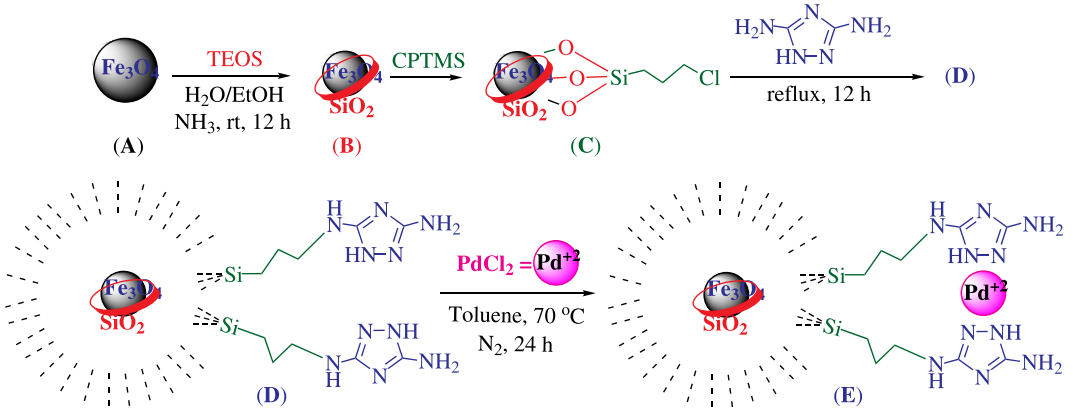

SCHEME 1 Synthesis of novel Pd nano-catalyst

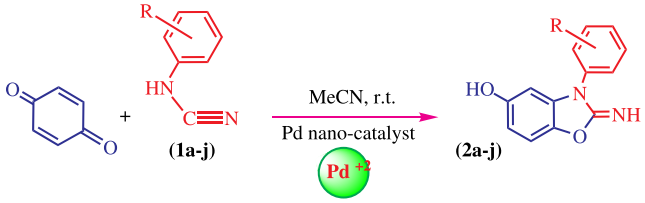

SCHEME 2 Synthesis of various 2-imino-3-aryl-2,3-dihydrobenzo[*d*]oxazol-5-ols

2.2 | Preparation of Pd nano-catalyst

A novel Pd nano-catalyst was prepared in the following five successive stages:

- Stage 1: Preparation of the Fe_3O_4 magnetic nanoparticles (Fe_3O_4 MNPs). The Fe_3O_4 MNPs was prepared according to the literature.[15] Briefly, the mixture of $FeCl_3.6H_2O$ (11.44 g) and $FeCl_2.4H_2O$ (4.3 g) was dissolved in water (100 ml), and the solution stirred for 0.5 h in 80 °C. The solution of 37% ammonia was then added dropwise with vigorous stirring which a black solid product obtained when a reaction media reached to pH 10. The mixture was heated for 0.5 h at 70 °C and the black magnetite solid product filtered, washed with water and dried at 80 °C for 12 h.
- Stage 2: Coating of the Fe_3O_4 magnetic nano-particles with SiO_2 (Fe_3O_4@SiO_2). Fe_3O_4@SiO_2 was synthesized according to the literature.[16] Briefly, Fe_3O_4 MNPs (0.2 g, prepared in the Stage 1) were dispersed into a solution containing ethanol and distilled water (250 ml, V/V = 4:1) and $NH_3.H_2O$ (3 ml) under ultrasonication. Then, tetraethyl orthosilicate (TEOS, 2 ml) was slowly added dropwise and the mixture stirred for further 6 h. Fe_3O_4@SiO_2 was obtained by centrifugation, washed with water and ethanol for several times, and dried in vacuo.
- Stage 3: Functionalization of the coated Fe_3O_4 with 3-chloropropyltrimethoxysilane (CPTMS) ligand (Fe_3O_4@SiO_2@CPTMS). (3-Chloropropyl) trimethoxysilane (CPTMS) (1.0 ml, 5 mmol) dissolved in dry toluene (100 ml) and Fe_3O_4@SiO_2 (1.0 g, prepared in the Stage 2) added and stirred for 18 h at 60 °C. Then, the obtained product was separated with strong magnet, washed with toluene and dried in vacuo.
- Stage 4: Further functionalization with 3,5-diamino-1,2,4-triazole (DAT) ligand (Fe_3O_4@SiO_2@CPTMS @DAT). 3,5-Diamino-1,2,4-triazole (DAT, 0.495 g, 5 mmol) and K_2CO_3 (0.69 g, 5 mmol) in toluene (60 ml) were added to Fe_3O_4@SiO_2@CPTMS (0.1 g, prepared in the Stage 3) and refluxed for 12 h. Then, the obtained product was separated with strong magnet, washed repeatedly with ethanol and water and dried in vacuo, and
- Stage 5: Complexation of Fe_3O_4@SiO_2@CPTMS@DAT with $PdCl_2$ (Fe_3O_4@SiO_2@CPTMS@DAT@Pd). Fe_3O_4@SiO_2@CPTMS@DAT (0.1 g, prepared in the Stage 4) was added to a dispersed $PdCl_2$ (0.88 g, 5 mmol) in toluene and stirred vigorously for 24 h under nitrogen atmosphere at 70 °C. Then, the resulting Pd catalyst was separated with strong magnet, washed with ethanol and air-dried.

2.3 | General Procedure for the synthesis of 2-imino-3-phenyl-2,3-dihydrobenzo[d] oxazol-5-ol derivatives

p-Benzoquinone (0.108 g, 1.0 mmol), the requisite phenylcyanamide (1.0 mmol) and the Pd nano-particle catalyst (20 mg) were combined in acetonitrile (5 ml). The mixture was stirred at room temperature and completion of the reaction monitored with TLC. Then, the Pd catalyst was separated by a magnet, the solid washed with acetone, the solvent removed *in vacuo* and the obtained solid recrystallized in ethanol.

3 | RESULTS AND DISCUSSION

3.1 | Characterization of the catalyst

Formation of the Pd nano-catalyst was verified using the CHN analysis, inductively coupled plasma (ICP), FT-IR, X-ray diffraction (XRD), dispersive X-ray spectroscopy (EDX), scanning electron microscopy (SEM), transmission electron microscopy (TEM), thermogravimetric-differential thermal analysis (TGA-DTA) and vibrating sample magnetometer (VSM).

3.1.1 | Characterization of the Pd catalyst by elemental analysis (CHN) and ICP

The elemental analysis report for the C, H and N elements was about 7.74, 0.32 and 1.98 respectively. The ICP analysis of the catalyst showed that the Pd content of Fe_3O_4@SiO_2@CPTMS@ DAT@Pd was about 35%.

3.1.2 | Characterization of the catalyst by IR spectroscopy

Figure 1 shows the five FT-IR spectra of **A**) Fe_3O_4 MNPs, **B**) Fe_3O_4@SiO_2, **C**) Fe_3O_4@SiO_2@CPTMS, **D**) Fe_3O_4@SiO_2@CPTMS@DAT and **E**) Fe_3O_4@SiO_2@CPTMS@DAT@Pd. Curve **A** exhibits basic characteristic peak at about 575 cm^{-1} which is attributed

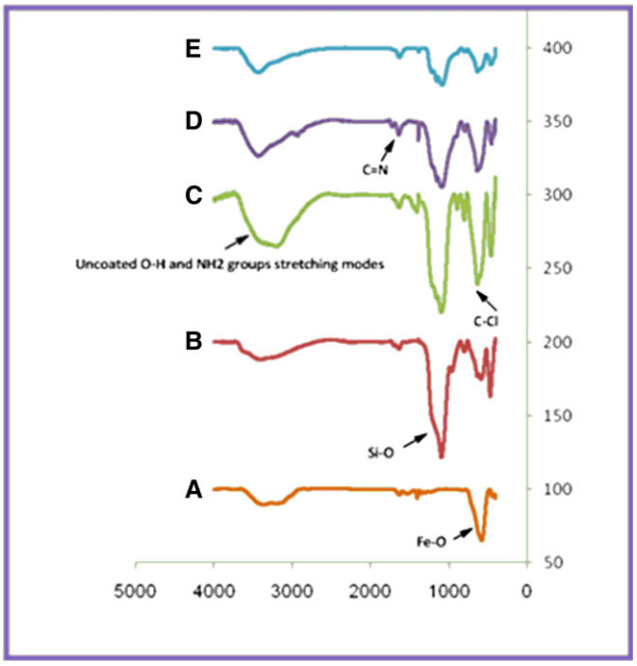

FIGURE 1 Comparison of the FT-IR spectra of five compounds (**A**, **B**, **C**, **D** and **E**)

to the presence of the Fe–O stretching vibrations. Curve **B** shows a broad band near 1100 cm^{-1} which indicates the silica coated magnetite nanoparticles. Curve **C** shows a new peak at about 635 cm^{-1} indicating presence of the C-Cl bond. Curve **D** shows two new peaks at 1384 and 1638 cm^{-1} which are attributed to the C-N and C=N bonds, respectively. Curve **E** shows a shift from 1638 to 1627 cm^{-1} which is related to the new interaction of Pd with the nitrogen of the C=N bond. Consequently, comparison of the IR spectra confirms the successful stages of the catalyst preparation, namely preparation of Fe_3O_4 MNPs, modification, functionalization and complexation.

3.1.3 | Characterization of the catalyst by the XRD patterns

The XRD pattern (Figure 2, **B**, blue) at about 2θ = 10, 30, 35, 45, 53, 57, 63 and 74, confirms the silica-coated magnetite nanoparticles (Fe_3O_4@SiO_2) structure. Appearance of the new peaks at 2θ =~37,~50,~70 and 87 are attributed to the Pd species (Figure 2, **E**, purple).[17]

3.1.4 | Characterization of the catalyst by the EDX analysis

The chemical composition of the Pd nano-catalyst was determined by the EDX analysis (Figure 3). The results confirm the presence of the anticipated elements in the structure of the catalyst, namely C (12.41 %), N (3.34 %), O (22.41 %), Si (2.99 %), Fe (11.33 %) and Pd (28.53 %).

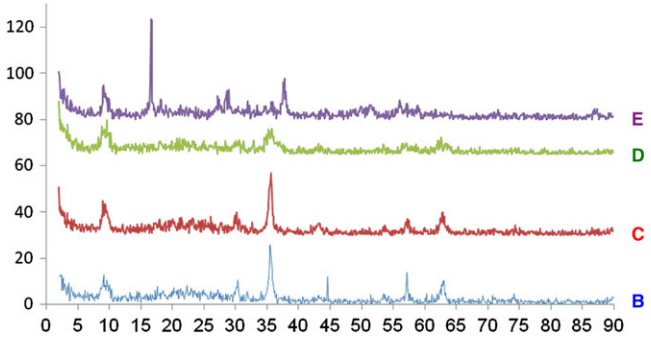

FIGURE 2 The XRD patterns of Fe_3O_4@SiO_2 (blue), Fe_3O_4@SiO_2@CPTMS (red), Fe_3O_4@SiO_2@CPTMS@DAT (green) and Fe_3O_4@SiO_2@CPTMS@DAT@Pd (purple)

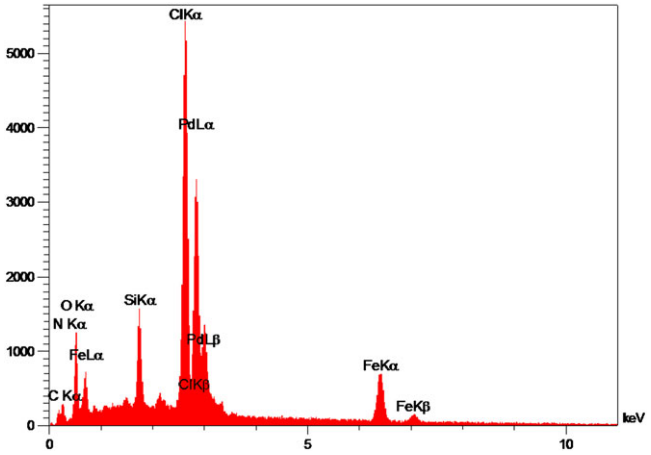

FIGURE 3 The EDX analysis of the catalyst

3.1.5 | Characterization of the catalyst by the SEM and the TEM images

The morphology and the particle size of the Pd nano-catalyst were determined by the SEM and TEM images (Figure 4). According to these images, the sizes of the Pd nano-catalyst particles are in the nanometer ranges (between 26.61-88.74 nm).

3.1.6 | Characterization of the catalyst by the TGA-DTA technique

The thermo-gravimetric analysis curves of the catalyst show the mass loss of the organic materials as they decompose upon heating (Figure 5). It can be observed that the catalyst shows about five weight loss steps in the temperature ranges of 145, 245, 340, 400 and 450 °C, respectively. The initial weight loss at 145 °C is probably due to the residual water, the second step at 245 °C is attributed to the thermal decomposition of the complex, the third step is probably due to the thermal decomposition of DAT and CPTMS ligands, the forth weight loss is

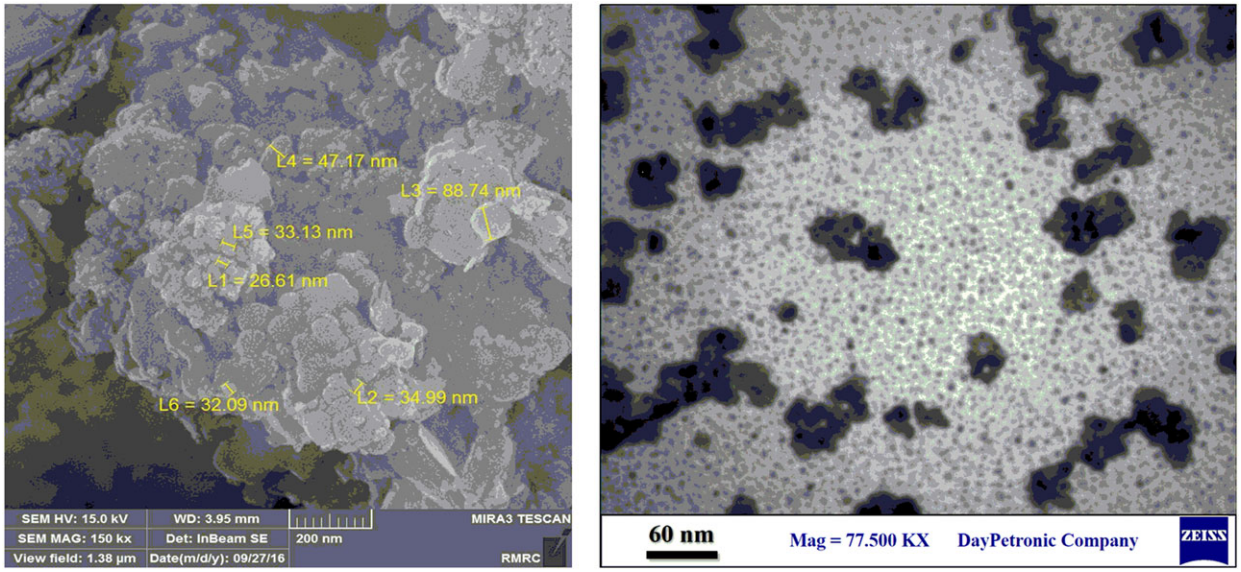

FIGURE 4 The SEM (left) and the TEM (right) images of the catalyst

related to the thermal decomposition of the SiO_2 coating layer and the fifth weight loss is attributed to the thermal decomposition of Fe_3O_4. On the basis of these results, modification and the well grafting of ligand groups is verified and indicated that the Pd catalyst has approximately a good thermal stability which is probably due to the strong interactions between the SiO_2 coating layer, the ligands and the Fe_3O_4 magnetic nano particles.

3.1.7 | Characterization of the catalyst by the VSM technique

The VSM analyses of the five compounds namely A) Fe_3O_4 MNPs, B) Fe_3O_4@SiO_2, C) Fe_3O_4@SiO_2@CPTMS, D) Fe_3O_4@SiO_2@CPTMS@DAT, and E) the Fe_3O_4@SiO_2@CPTMS@DAT@Pd nano-catalyst were performed in order to demonstrate and compare their magnetic properties (Figure 6). As can be seen, all five compounds have magnetic properties; and show a nice decrease from A to E (70, 35, 30, 27 and 12 emu/g, respectively). This can be explained by considering the probable reduction in the dipolar–dipolar interactions between the magnetic nanoparticles after their modification and complexation which cause the more coating of Fe_3O_4 MNPs.

3.2 | Optimization

The catalyst activity was investigated in a model reaction for the synthesis of 3-(2,5-dichlorophenyl)-2-imino-2,3-dihydrobenzo[*d*]oxazol-5-ol from the reaction of *p*-benzoquinone with 2,5-dichlorophenyl- cyanamide under different conditions of temperature, amount of the catalyst and solvent. The best result was obtained with 1.0 mmol of 1: 1 of *p*-benzoquinone: 2,5-dichlorophenylcyanamide with 20 mg of the Pd nano-particle catalyst in acetonitrile at room temperature (Table 1).

3.3 | Synthesis of various 2-imino-3-phenyl-2,3-dihydrobenzo[*d*]oxazol-5-ol derivatives

Applying the optimized results from the model reaction, various 2-imino-3-phenyl-2,3-dihydro- benzo[*d*]oxazol-5-ol derivatives were synthesized from the reaction of benzoquinone with phenylcyanamides in acetonitrile at room temperature with good to excellent yields (Table 2). As can be seen, those phenylcyanamides with electron donating groups require shorter reaction times.

3.4 | Characterization of the 2-imino-3-phenyl-2,3-dihydrobenzo[*d*]oxazol-5-ols

All known compounds were characterized by comparing their physical and spectroscopic data with those reported in the literature. The structures of all products were in agreement with their IR and NMR spectra. In the IR spectra, the sharp N-H (about 3300 cm^{-1}) and C≡N (about 2300 cm^{-1}) peaks disappeared and were replaced by strong absorption bands for O-H stretching at 3300 cm^{-1}. Peaks at 1680 and 1000-1100 cm^{-1} can be attributed to the new formed C=N and C-O bands, respectively.

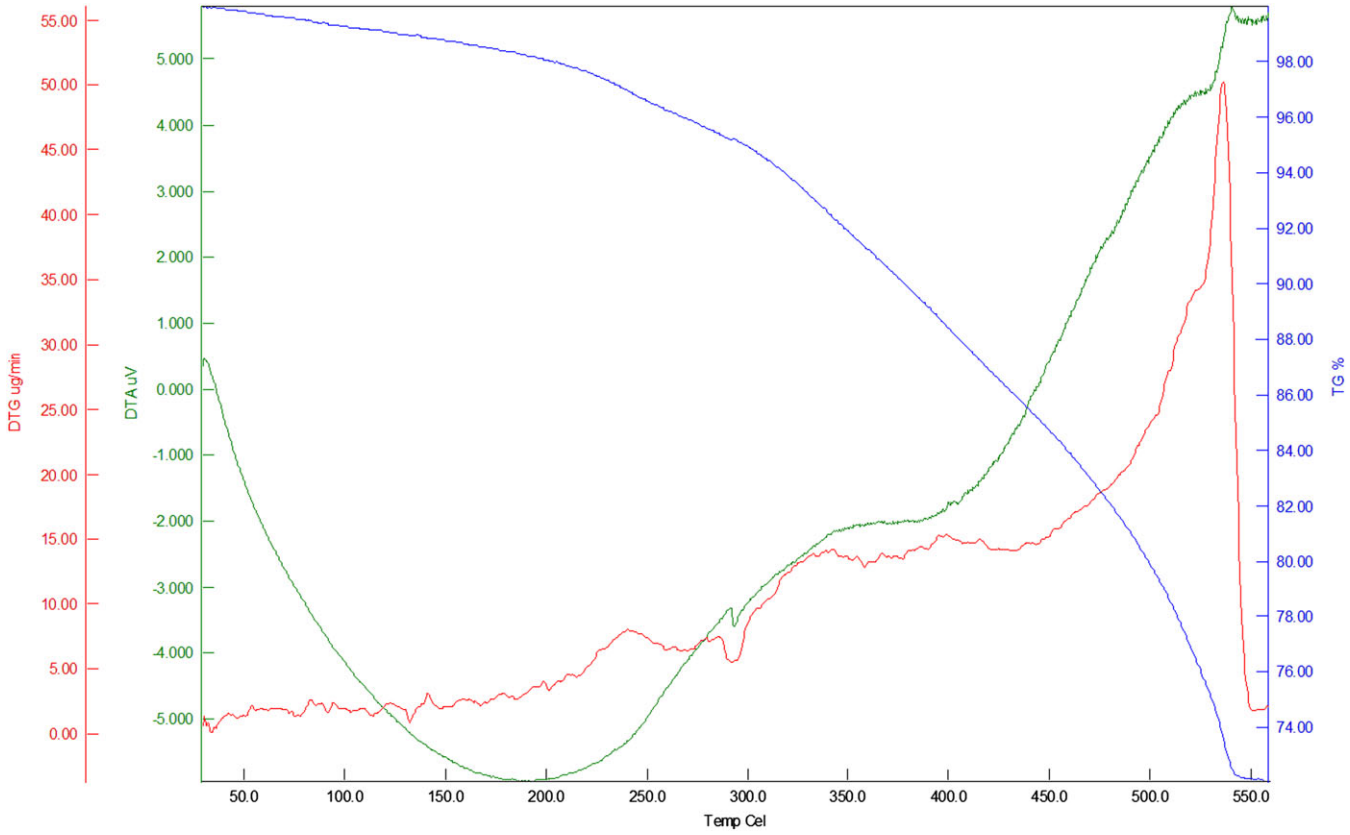

FIGURE 5 TGA-DTA patterns of the catalyst in N_2 atmosphere

3.5 | Selected spectral data

3.5.1 | 3-(2-Chlorophenyl)-2-imino-2,3-dihydrobenzo[d]oxazol-5-ol (2a)

M.p. 199-202 °C, FT-IR (KBr, cm^{-1}): 3329, 3068, 1687, 1620, 1589, 1497, 1477, 1439, 1406, 1306, 1189, 1108, 1066, 1010, 838, 818, 768, 721, 703, 658, 620; ^{1}H NMR (DMSO-d_6, 300 MHz): δ = 9.26 (br, 1H), 7.73 (t, J = 4.4, 1H), 7.66 (t, J = 4.4, 3H), 7.55 (t, J = 4.4, 2H), 7.03 (d, J = 8.4, 1H), 6.40 (d, J= 8.4, 1H), 5.95 (s, 1H); ^{13}CNMR (DMSO-d_6, 75 MHz,): δ = 155.2, 154.5, 137.5, 134.1, 132.7, 132.2, 131.6, 131.4, 131.2, 129.3, 109.6, 107.6, 96.4; CHN: Anal. Calcd for $C_{13}H_9N_2O_2Cl$: C, 59.86; H, 3.08; N, 10.75. Found: C, 59.90; H, 3.48; N, 10.75.

3.5.2 | 3-(2,5-Dichlorophenyl)-2-imino-2,3-dihydrobenzo[d]oxazol-5-ol (2b)

M.p. 231-234 °C., FT-IR (KBr, cm^{-1}): 3332, 3096, 2683, 1681, 1621, 1601, 1560, 1490, 1476, 1426, 1401, 1306, 1194, 1099, 1014, 848, 826, 784, 712, 661, 613, 582, 438. ^{1}H NMR (DMSO-d_6, 300 MHz): δ = 8.00-7.40 (m, 3H), 7.25 (br, 1H), 6.97 (d, J = 8.1, 1H), 6.72 (br, 1H), 6.35 (d, J = 8.1, 1H), 5.96 (s, 1H); ^{13}C NMR (DMSO-d_6, 75 MHz,): δ = 154.6, 154.4, 137.4, 133.6, 133.0, 132.4, 131.5, 131.3, 129.4, 127.6, 109.6, 107.7, 96.5; CHN: Anal. Calcd for $C_{13}H_8N_2O_2Cl_2$: C, 51.78; H, 2.62; N, 8.82. Found: C, 52.91; H, 2.73; N, 9.49.

3.5.3 | 3-(4-Chlorophenyl)-2-imino-2,3-dihydrobenzo[d]oxazol-5-ol (2c)

M.p. 210-212 °C, FT-IR (KBr, cm^{-1}): 3361, 3088, 1674, 1620, 1499, 1466, 1382, 1275, 1188, 1159, 1087, 1003, 970, 811, 713, 628; ^{1}HNMR (300 MHz, DMSO-d_6): δ = 9.35 (br, 1H), 7.61 (q, J = 8.8, 4H), 7.00 (d, J = 8.4, 1H), 6.60 (br, 1H), 6.45 (d, J = 8.4, 1H), 6.37 (s, 1H); ^{13}CNMR (75 MHz, DMSO-d_6): δ = 155.2, 154.4, 137.3, 134.2, 133.4, 132, 129.9, 127.9, 109.5, 107.8, 96.6; CHN: Anal. Calcd for C13H9N2O2Cl: C, 60.45; H, 3.24; N, 10.96. Found: C, 59.90; H, 3.48; N, 10.75.

3.5.4 | 3-(2,4-Dichlorophenyl)-2-imino-2,3-dihydrobenzo[d]oxazol-5-ol (2d)

M.p. 216-218 °C, FT-IR (KBr, cm^{-1}): 3333, 3100, 2875, 2683, 1678, 1618, 1587, 1561, 1487, 1473, 1306, 1251, 1216, 1192, 1163, 1029, 1017, 898, 818, 778, 711, 677, 616, 563, 541, 441, 408; ^{1}H NMR (300 MHz, DMSO-d_6): δ = 7.93(s, 1H), 7.80, (m, 1H), 7.62 (s, 1H), 7.30, (s, 1H),

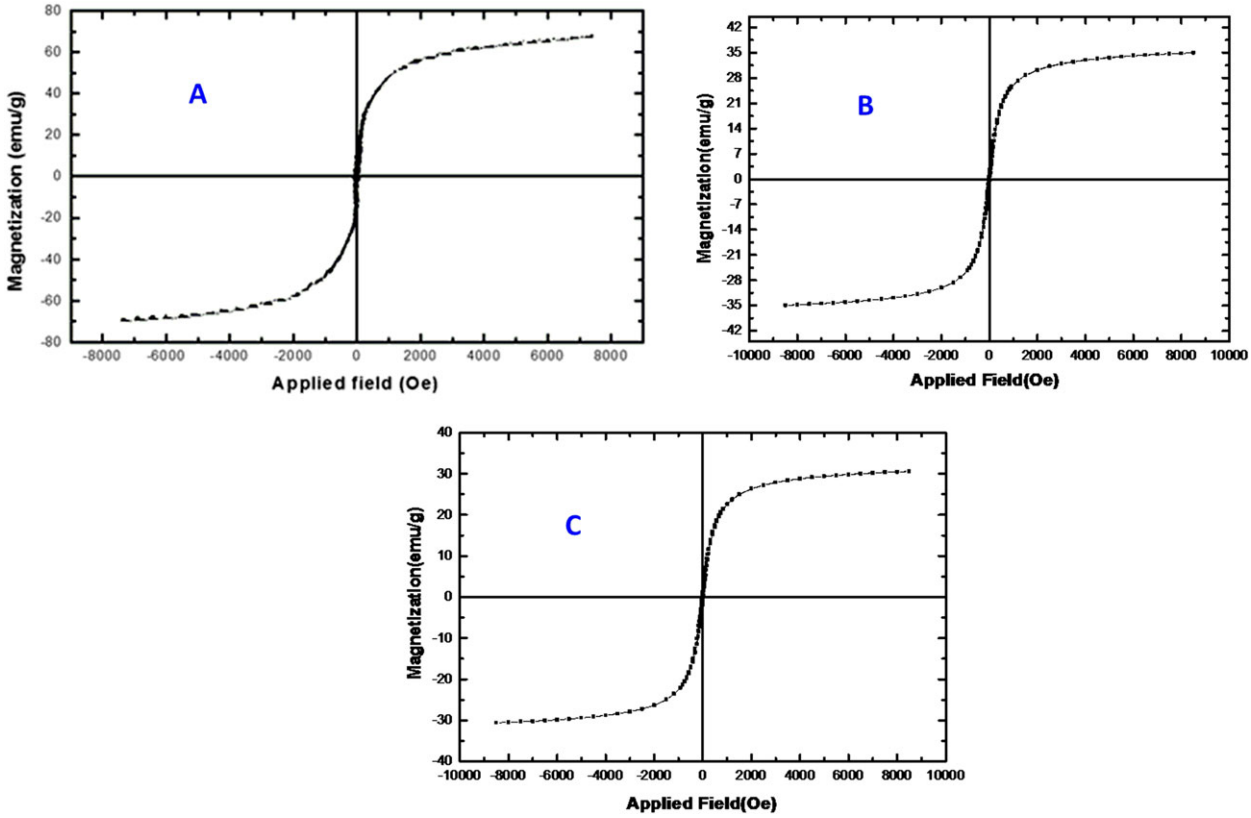

FIGURE 6 The VSM analyses of **A**, **B**, **C**, **D** and **E**

7 (d, $J = 8.4$, 1H), 6.90 (br, 1H), 6.40 (d, $J = 8.4$); ^{13}C NMR (DMSO-d_6, 75 MHz): δ = 154.6, 154.3, 137.1, 135.5, 132.8, 131.6, 129.7, 129.4, 127.9, 125.9, 109.6, 108.1, 96.8; CHN: Anal. Calcd for $C_{13}H_8N_2O_2Cl_2$: C, 52.34; H, 2.37; N, 8.91. Found: C, 52.91; H, 2.73; N, 9.49.

3.5.5 | 3-(3-Bromophenyl)-2-imino-2,3-dihydrobenzo[d]oxazol-5-ol (2e)

M.p. 164-167 °C, FT-IR (KBr, cm^{-1}): 3330, 3065, 1674, 1618, 1590, 1488, 1478, 1438, 1394, 1307, 1199, 1168, 1116, 1073, 1014, 780, 744, 724, 713, 699, 653, 624. ^{1}H NMR (DMSO-d_6, 300 MHz): δ = 9.40 (br, 1H), 7.64-7.48 (m, 3H), 7.00 (d, $J = 8.5$, 1H), 6.80 (br, 1H), 6.41 (d, $J = 8.2$ Hz, 2H); ^{13}C NMR (DMSO-d_6, 75 MHz): δ = 154.4, 154.7, 137.3, 136.9, 133.2, 131.7, 130.5, 128.9, 124.9, 122.2, 109.6, 107.9, 96.6; CHN: Anal. Calcd for $C_{13}H_9N_2O_2Br$: C, 51.45; H, 2.70; N, 9.26. Found: C, 51.17; H, 2.97; N, 10.49.

3.5.6 | 2-Imino-3-p-tolyl-2,3-dihydrobenzo[d]oxazol-5-ol (2f)

M.p. 207-209 °C, FT-IR (KBr, cm^{-1}): 3360, 3064, 1675, 1618, 1580, 1516, 1494, 1475, 1442, 1408, 1382, 1272, 1225, 1000, 998, 970, 821, 811, 793, 713, 689, 646, 619,

TABLE 1 Optimization of the reaction

Entry	*p*-Benzoquinone[a]	Amount of catalyst	Solvent	Time (min)	Yield %
1	1.5 mmol	40 mg	EtOH	50[b]	20
2	1.5 mmol	30 mg	MeOH	50[b]	12
3	**1.0 mmol**	**20 mg**	**MeCN**	**8**[c]	**82**
4	1.5 mmol	30 mg	MeCN	10[b]	40
5	1.0 mmol	40 mg	MeCN	12[d]	35

[a]2,5-Dichlorophenylcyanamide (1 mmol),

[b]reflux,

[c]room temperature, and

[d]at 50 °C.

TABLE 2 Synthesis of various 2-imino-3-phenyl-2,3-dihydrobenzo[*d*]oxazol-5-ols

Entry	Phenylcyanamide	Product	Time (min)	Yield (%)
1	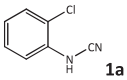 1a	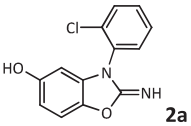 2a	110	88
2	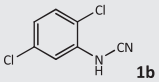 1b	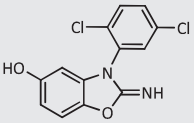 2b	450	82
3	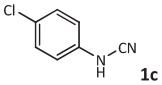 1c	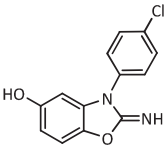 2c	250	90
4	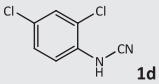 1d	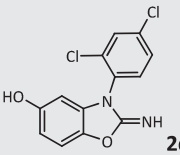 2d	150	80
5	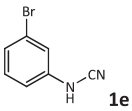 1e	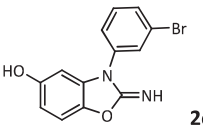 2e	120	80
6	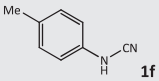 1f	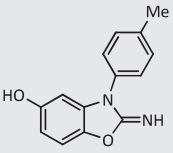 2f	70	82
7	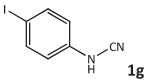 1g	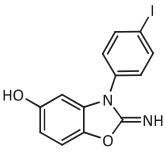 2g	250	92
8	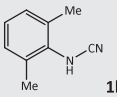 1h	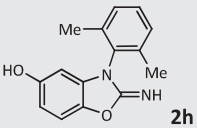 2h	25	87
9	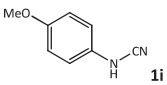 1i	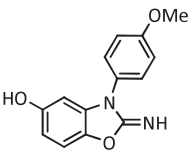 2i	100	85
10	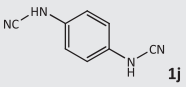 1j	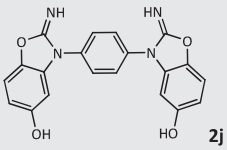 2j	35	78

608; ^{1}H NMR (DMSO-d_6, 300 MHz): δ = 9.35 (br, 1H), 7.37 (d, J = 7.6, 2H), 7.34 (d, J = 7.6, 2H), 6.99 (d, J = 8.4, 1H), 6.40 (d, J = 8.4, 1H), 6.30 (s, 1H), 2.35 (s, 3H); ^{13}C NMR (DMSO-d_6, 75 MHz): δ = 155.9, 154.5, 137.7, 137.7, 137.3, 134.1, 132.6, 130.5, 126.1, 109.4, 107.6, 96.4, 21.1; CHN: Anal. Calcd for $C_{14}H_{12}N_2O_2$: C, 69.31; H, 4.76; N, 11.45. Found: C, 69.99; H, 5.03; N, 11.66.

3.5.7 | 2-Imino-3-(4-iodophenyl)-2,3-dihydrobenzo[d]oxazol-5-ol (2g)

M.p. 248-251 °C, FT-IR (KBr, cm^{-1}): 3358, 3059, 1676, 1627, 1617, 1583, 1566, 1499, 1404, 1381, 1273, 1190, 1158, 1058, 1001, 969, 820, 711, 684, 634, 622, 501; ^{1}H NMR (DMSO-d_6, 300 MHz): δ = 9.33 (br, 1H), 7.88 (d, J = 8.1, 2H), 7.41 (d, J = 8, 2H), 6.99 (d, J = 8.4, 1H), 6.70 (br, 1H), 6.39 (t, J = 8.8, 2H); ^{13}C NMR (DMSO-d_6, 75 MHz): δ = 155.1, 154.3, 138.8, 137.3, 135.2, 133.3, 128.2, 109.5, 107.9; CHN: Anal. Calcd for $C_{13}H_9N_2O_2I$: C, 44.64; H, 2.40; N, 8.22. Found: C, 44.34; H, 2.58; N, 7.96.

3.5.8 | 3-(2,6-Dimethylphenyl)-2-imino-2,3-dihydrobenzo[d]oxazol-5-ol (2h)

M.p. 204-207 °C, FT-IR (KBr, cm^{-1}): 3347, 3315, 2954, 1862, 2688, 1679, 1616, 1475, 1379, 1296, 1178, 1101, 1003, 837, 798, 778, 728, 709, 634, 446; ^{1}H NMR (DMSO-d_6, 300 MHz): δ = 9.30 (br, 1H), 7.27 (br, 3H), 7.02 (d, J = 8.2, 1H), 6.43 (br, 1H), 6.36 (d, J = 7.57, 1H), 5.79 (d, J = 2.33, 1H), 2.07 (s, 6H); ^{13}C NMR (DMSO-d_6, 75 MHz): δ = 154.7, 154.2, 137.7, 133.9, 132.2, 129.5, 129.1, 109.5, 107.1, 95.6, 17.7; CHN: Anal. Calcd for $C_{15}H_{14}N_2O_2$: C, 69.95; H, 5.33; N, 10.84. Found: C, 70.85; H, 5.55; N, 11.02.

3.5.9 | 2-Imino-3-(4-methoxyphenyl)-2,3-dihydrobenzo[d]oxazol-5-ol (2i)

M.p. 177-180 °C, FT-IR (KBr, cm^{-1}): 3336, 3089, 1673, 1617, 1579, 1499, 1479, 1414, 1294, 1196, 1161, 1090, 1011, 969, 833, 811, 744, 706, 625, 501; ^{1}H NMR (DMSO-d_6, 300 MHz): δ = 9.30 (b, 1H), 7.45 (d, J = 8.4, 2H), 7.90 (d, J = 7.8, 2H), 6.98 (d, J = 8.4, 1H), 6.55 (br, 1H), 6.34 (d, J = 8.1, 1H), 6.18 (s, 1H); ^{13}C NMR (DMSO-d_6, 75 MHz): δ = 158.9, 155.5, 154.3, 137.2, 134.4, 127.9, 115.2, 109.3, 107.2, 96.1, 55.8; CHN: Anal. Calcd for $C_{14}H_{12}N_2O_3$: C, 65.36; H, 4.61; N, 11.11. Found: C, 65.62; H, 4.72; N, 10.93.

3.5.10 | 3,3′-(1,4-Phenylene)bis(2-imino-2,3-dihydrobenzo[d]oxazol-5-ol) (2j)

M.p. 231-234 °C, FT-IR (KBr, cm-1): 3329, 3069, 1674, 1618, 1521, 1480, 1396, 1292, 1190, 1161, 1110, 1007, 971, 810, 715, 640, 521; ^{1}H NMR (DMSO-d_6, 300 MHz): δ = 9.35 (b, 2H), 7.77 (s, 4H), 7.15-6.50 (m, 4H), 6.40 (d, J = 8.1 Hz, 4H); ^{13}C NMR (DMSO-d_6, 75 MHz): δ = 154.9., 154.4, 137.3, 134.0, 133.5, 127.1, 109.5, 107.7, 96.5; CHN: Anal. Calcd for $C_{20}H_{14}N_4O_4$: C, 63.58; H, 3.35; N, 14.24. Found: C, 64.17; H, 3.77; N, 14.97.

3.5.11 | 3-(2,4-Dichlorophenyl)-2-imino-2,3-dihydrobenzo[d]ox-azol-5-yl 4-methylbenzenesulfonate (3d)

Yield 85%; mp 164-166 °C; FT-IR (KBr, cm^{-1}): 3339, 3038, 1711, 1693, 1597, 1491, 1476, 1369, 1221, 1194, 1171, 1130, 1093, 1078, 1163, 999, 900, 853, 812, 797, 748, 723, 666, 649, 632, 598, 553; ^{1}H NMR (DMSO-d_6, 400 MHz): δ = 7.72 (d, J = 8.0 Hz, 2H), 7.67 (d, J = 8.4 Hz, 2H), 7.44-7.41 (dd, J = 2.4, 2.0 Hz, 1H), 7.37 (d, J = 8.0 Hz, 3H), 7.19 (d, J = 8.8 Hz, 1H), 6.77-6.75 (d, J = 8.8 Hz, 1H), 6.61 (d, J = 2.4 Hz, 1H), 2.49 (s, 3H); ^{13}C NMR (DMSO-d_6, 100 MHz): δ = 156.4, 145.9, 145.8, 142.8, 134.1, 133.2, 132.6, 132.4, 131.9, 131.8, 129.9, 128.6, 127.7, 125.2, 117.0, 110.1, 104.0, 21.8; CHN: Anal. Calcd for C20H14Cl2N2O4S: C, 53.46; H, 3.14; N, 6.23. Found: C, 53.81; H, 3.21; N, 6.32.

3.5.12 | 3-(3-Bromophenyl)-2-imino-2,3-dihydrobenzo[d]oxazol-5-yl 4-methylbenzenesulfonate (3e)

Yield 87%; mp 189-190 °C; FT-IR (KBr, cm^{-1}): 3334, 3086, 1702, 1590, 1495, 1478, 1430, 1388, 1363, 1221, 1192, 1171, 1135, 1092, 1071, 996, 888, 868, 850, 818, 784, 742, 722, 700, 684, 665, 653, 617, 594, 554, 520; ^{1}H NMR (DMSO-d_6, 400 MHz): δ = 7.72 (d, J = 8.4 Hz, 2H), 7.64-7.61 (m, 2H), 7.45-7.44 (m, 2H), 7.37 (d, J = 8.4 Hz, 3H), 7.09 (d, J = 8.8 Hz, 1H), 6.69 (d, J = 8.8 Hz, 1H), 6.59 (d, J = 2.4 Hz, 1H), 2.49 (s, 3H); ^{13}C NMR (DMSO-d_6, 100 MHz): δ = 156.2, 145.7, 145.6, 142.9, 135.3, 133.2, 131.9, 131.6, 131.3, 129.9, 128.7, 128.6, 124.2, 123.3, 116.1, 109.4, 103.5, 21.8; CHN: Anal. Calcd for $C_{20}H_{15}BrN_2O_4S$: C, 52.30; H, 3.29; N, 6.10. Found: C, 52.42; H, 3.37; N, 6.21.

3.5.13 | 3-(4-Iodophenyl)-2-imino-2,3-dihydrobenzo[d]oxazol-5-yl 4-methylbenzenesulfonate (3f)

Yield 84%; mp 199-201 °C; FT-IR (KBr, cm^{-1}): 3344, 3043, 1704, 1496, 1480, 1355, 1170, 1132, 1092, 893, 857, 819, 753, 592, 553; ^{1}H NMR (DMSO-d_6, 400 MHz): δ = 7.89 (d, J = 8.4 Hz, 2H), 7.72 (d, J = 8.0 Hz, 2H), 7.36 (d, J = 8.0 Hz, 3H), 7.24 (d, J = 8.4 Hz, 2H), 7.09 (d, J = 8.8 Hz, 1H), 6.66 (d, J = 8.8 Hz, 1H), 6.58 (d, J = 2.4 Hz, 1H), 2.50 (s, 3H); ^{13}C NMR (DMSO-d_6, 100 MH): δ = 156.2, 145.7, 145.6, 142.9, 139.2, 133.7, 133.2, 131.9, 129.9, 128.7, 127.2, 116.0, 109.4, 103.6, 93.4, 21.8; CHN: Anal. Calcd for C20H15IN2O4S: C, 47.44; H, 2.99; N, 5.53. Found: C, 47.52; H, 3.10; N, 5.64.

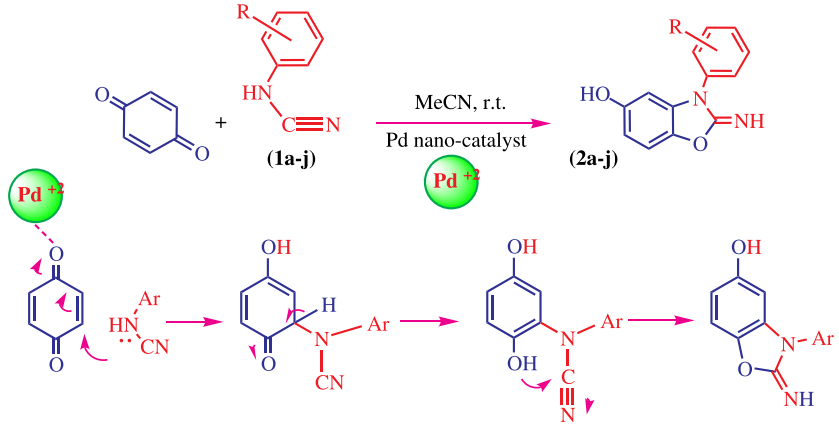

SCHEME 3 Suggested mechanism for the synthesis of 2-imino-3-aryl-2,3-dihydrobenzo[*d*]oxazol-5-ols

3.5.14 | 3-(2,6-Dimethylphenyl)-2-imino-2,3-dihydrobenzo[d]ox-azol-5-yl 4-methylbenzenesulfonate (3g)

Yield 86%; mp 121-123 °C; FT-IR (KBr, cm^{-1}): 3329, 3052, 1699, 1609, 1490, 1369, 1212, 1191, 1172, 1091, 988, 956, 864, 840, 822, 722, 745, 665, 652, 630, 599, 556, 525; ^{1}H NMR (DMSO-d_6, 400 MHz): δ = 7.68 (d, J = 8.4 Hz, 2H), 7.36 (t, J = 7.6 Hz, 1H), 7.31 (d, J = 8.4 Hz, 2H), 7.25 (d, J = 7.6 Hz, 2H), 7.16 (d, J = 8.8 Hz, 3H), 6.73 (d, J = 8.8 Hz, 1H), 6.17 (d, J = 2.4 Hz, 1H), 2.46 (s, 3H), 2.09 (s, 6H); ^{13}C NMR (DMSO-d_6, 100 MHz): δ = 156.8, 145.9, 145.6, 143.0, 137.2, 133.2, 131.8, 130.3, 129.8, 129.6, 129.4, 128.6, 115.9, 109.8, 103.2, 21.7, 17.7; CHN: Anal. Calcd for $C_{22}H_{20}N_2O_4S$: C, 64.69; H, 4.94; N, 6.86. Found: C, 64.78; H, 4.86; N, 6.94.

3.5.15 | 3,3'-(1,4-Phenylene)bis(2-imino-2,3-dihydrobenzo[d]ox-azole-5,3-diyl)bis(4-methylbenzene- sulfonate) (3h)

Yield 85%; mp 115 °C dec; FT-IR (KBr, cm^{-1}): 3338, 3067, 1705, 1617, 1598, 1519, 1485, 1454, 1381, 1292, 1257, 1219, 1193, 1180, 1132, 1091, 991, 956, 895, 862, 835, 814, 742, 664, 594, 552, 529; ^{1}H NMR (DMSO-d_6, 400 MHz): δ = 7.76 (d, J = 8.4 Hz, 4H), 7.66 (s, 4H), 7.39 (d, J = 8.4 Hz, 6H), 7.04 (d, J = 8.8 Hz, 2H), 6.72 (s, 2H), 6.67 (d, J = 8.8 Hz, 2H), 2.50 (s, 6H); ^{13}C NMR (DMSO-d_6, 100 MHz): δ = 156.2, 145.7, 145.5, 142.9, 133.7, 133.2, 132.0, 129.9, 128.7, 126.7, 116.1, 109.4, 103.7, 21.8; CHN: Anal. Calcd for $C_{34}H_{26}N_4O_8S_2$: C, 59.81; H, 3.84; N, 8.21. Found: C, 59.90; H, 3.87; N, 8.27.

3.6 | The plausible mechanism

The plausible mechanism for the synthesis of various 2-imino-3-phenyl-2,3-dihydrobenzo[*d*]oxazol-5-ol from the reaction of benzoquinone with different phenylcyanamides at room temperature under solvent-free conditions is shown in the presence of the Pd nano-catalyst (Scheme 3). The proposed mechanism is probably due to the Lewis acidity of the Pd nano-catalyst by attaching to the carbonyl group to facilitate the nucleophilic attack of the nitrogen atom to form the intermediate with the subsequent cyclization to get the final product.

3.7 | The reusability of the Pd nano-catalyst

Recovery and reusability of the catalyst are important aspects, so the recyclability of the Pd nano-catalyst (Fe_3O_4@SiO_2@CPTMS@DAT@Pd) was investigated in a model reaction (synthesis of 3-(2,5-dichlorophenyl)-2-imino-2,3-dihydrobenzo[*d*]oxazol-5-ol from the reaction of *p*-benzoquinone (1.0 mmol) with 2,5-dichlorophenylcyanamide (1.0 mmol) with 20 mg of the Pd nano-particle catalyst in acetonitrile at room temperature. Therefore, the catalyst was separated by filtration after the first run, washed with ethanol and dried at 120 °C under vacuum and then used for the next successive runs under the same conditions. No significant loss of the activity was observed, indicating that the applied catalyst is capable and has the high stability during the synthesis of various 2-imino-3-phenyl-2,3-dihydrobenzo[*d*]oxazol-5-ols.

4 | CONCLUSION

In conclusion, a novel Pd nano-catalyst was successfully prepared, characterized and applied for the synthesis of a range of 2-imino-3-phenyl-2,3-dihydrobenzo[*d*]oxazol-5-ols.

ACKNOWLEDGEMENT

The authors are grateful to the Bu-Ali Sina University, Hamedan Iran, for the financial support of this work.

ORCID

Davood Habibi http://orcid.org/0000-0002-2386-8502

REFERENCES

[1] T. Li, Y. Liu, F.-S. Liu, *Appl. Clay Sci.* **2017**, *136*, 18.

[2] S. M. Ghodse, V. N. Telvekar, *Tetrahedron Lett.* **2017**, *58*, 524.

[3] R. Manikandan, P. Anitha, P. Viswanathamurthi, J. G. Maleck, *Polyhedron* **2016**, *119*, 300.

[4] A. Naghipour, A. Ghorbani-Choghamarani, H. Babaee, M. Hashemi, B. Notash, *J. Organomet. Chem.* **2017**, *841*, 31.

[5] W. Zawartka, A. Gniewek, A. M. Trzeciak, *Inorg. Chim. Acta* **2017**, *455*, 595.

[6] M. Sarmah, M. Mondal, S. B. Gohain, U. Bora, *Catal. Commun.* **2017**, *90*, 31.

[7] M. J. Bravo, R. M. Ceder, A. Grabulosa, G. Muller, M. Rocamora, M. Font-Bardia, *J. Organomet. Chem.* **2017**, *830*, 42.

[8] M. E. Martínez-Klimov, P. Hernandez-Hipólito, T. E. Klimova, D. A. Solís-Casados, M. Martínez-García, *J. Catal.* **2016**, *342*, 138.

[9] J. L. Tan, A. M. De Jesus, S. L. Chua, J. Sanetuntikul, S. Shanmugam, B. J. V. Tongol, H. Kim, *Appl. Catal. A-Gen.* **2017**, *531*, 29.

[10] P. S. Sinija, K. Sreekumar, *J. Mol. Catal. A-Chem.* **2015**, *407*, 87.

[11] C. Burda, X. Chen, R. Narayanan, M. A. El-Sayed, *Chem. Rev.* **2005**, *105*, 1025.

[12] R. Dey, N. Mukherjee, S. Ahammed, B. C. Ranu, *Chem. Commun.* **2012**, *48*, 7982.

[13] W. Hou, N. A. Dehm, R. W. J. Scott, *J. Catal.* **2008**, *253*, 22.

[14] J. A. Glaser, *Clean Techn. Environ. Policy.* **2012**, *14*, 513.

[15] D. Habibi, S. Heydari, A. Gil, M. Afsharfarnia, A. Faraji, R. Karamian, M. Asadbegy, *Appl. Organomet. Chem.* **2017**, https://doi.org/10.1002/aoc.4005.

[16] P. Wang, X. Wang, S. Yu, Y. Zou, J. Wang, Z. Chen, N. S. Alharbi, A. Alsaedi, T. Hayat, Y. Chen, X. Wang, *Chem. Eng. J.* **2016**, *306*, 280.

[17] https://www.researchgate.net/figure/6153079_fig2_Figure-2-X-ray-diffraction-pattern-of-palladium-nano -particles-prepared-with-PEI-CO-C.

SUPPORTING INFORMATION

Additional Supporting Information may be found online in the supporting information tab for this article.

How to cite this article: Habibi D, Heydari S, Afsharfarnia M, Moghimpour F. Preparation of novel palladium nanoparticles supported on magnetic iron oxide and their catalytic application in the synthesis of 2-imino-3-phenyl-2,3-dihydrobenzo[*d*]oxazol-5-ols. *Appl Organometal Chem*. 2018;e4263. https://doi.org/10.1002/aoc.4263